Gan, Guohui (2016) Dynamic thermal simulation of horizontal ground heat exchangers for renewable heating and ventilation of buildings. Renewable Energy, 103 . pp. 361-371. ISSN 1879-0682

Dynamic thermal simulation of horizontal ground heat exchangers for renewable heating and ventilation of buildings

Guohui Gan
Department of Architecture and Built Environment, University of Nottingham, University Park, Nottingham NG7 2RD, UK
Email: guohui.gan@nottingham.ac.uk

Abstract: A ground heat exchanger is used to transfer thermal energy stored in soil in order to provide renewable heating, cooling and ventilation of a building. A computer program has been developed for simulation of the dynamic thermal performance of horizontally coupled earth-liquid heat exchanger for a ground source heat pump and earth-air heat exchanger for building ventilation. Neglecting the dynamic interactions between a heat exchanger and environments would significantly over predict its thermal performance and in terms of the amount of daily heat transfer the level of over-prediction could be as much as 463% for an earth-liquid heat exchanger and more than 100% for an earth-air heat exchanger. The daily heat transfer increases with soil moisture and for an earth-liquid heat exchanger the increase is between 3% and 35% with increase in moisture from 0.22 to 0.3 m^3/m^3 depending on the magnitude of heat transfer. Heat transfer through a plastic earth-liquid heat exchanger can be increased by 10% to 12% if its thermal properties are improved to the same as surrounding soil. The increase is smaller between 2% and 4% for an earth-air heat exchanger. In addition, an earth-liquid heat exchanger is more efficient than an earth-air heat exchanger.

Keywords: ground heat exchanger, heat and moisture transfer, ground-source heat pump, earth-air ventilation, dynamic interaction

Nomenclature

C	specific heat of soil (J/kgK)
D	damping depth of annual temperature fluctuation (m)
d	internal diameter of heat exchanger pipe (m)
$D_{T,l}$	thermal liquid moisture diffusivity (m^2/sK)
$D_{T,v}$	thermal vapour moisture diffusivity (m^2/sK)
$D_{\Theta,l}$	isothermal liquid moisture diffusivity (m^2/s)
$D_{\Theta,v}$	isothermal vapour moisture diffusivity (m^2/s)
E	amount of daily heat transfer per unit length of heat exchanger (Wh/m)
h_c	convective heat transfer coefficient (W/m^2K)
K	hydraulic conductivity of soil (m/s)
k	thermal conductivity of soil (W/mK)
k_f	thermal conductivity of fluid in pipe (W/mK)
L	latent heat of vaporisation (J/kg)
l	pipe length (m)

Pr Prandtl number
q heat transfer rate per unit length of heat exchanger (W/m)
q_c convective heat transfer (W/m^2)
q_e latent heat transfer due to evaporation or condensation (W/m^2)
q_p sensible heat transfer due to precipitation (W/m^2)
q_r radiation heat transfer (W/m^2)
q_v volumetric heat production/dissipation rate (W/m^3)
Re Reynolds number
T soil temperature (^oC)
T_f fluid temperature in pipe (^oC)
T_m annual mean temperature of deep soil (^oC)
T_{amp} annual amplitude of soil surface temperature (^oC)
T_p temperature of the interior surface of pipe (^oC)
t time (s)
t_d time (day)
t_{dl} time lag from a starting date to the occurrence of the minimum temperature in a year (day)
V_e flow of moisture due to evaporation/condensation (m/s)
V_p flow of moisture due to precipitation (m/s)
Z depth from soil surface (m)
z vertical coordinate (m)

Θ volumetric moisture content (m^3/m^3)
Θ_v source/sink of moisture (m^3/m^3s)
ξ direction normal to boundary (m)
ρ soil density (kg/m^3)
ρ_l density of liquid water (kg/m^3)

Abbreviations
HX heat exchanger
EAHX earth-air heat exchanger
EATV earth-air tunnel ventilation
ELHX earth-liquid heat exchanger
GSHP ground source heat pump

1 Introduction

A ground coupled heat exchanger is employed to transfer heat or coolth between the fluid within the heat exchanger and surrounding soil with a relatively stable temperature for a number of renewable energy-efficient systems including earth-air tunnel ventilation for preheating or cooling of supply air to a building, ground source and wastewater source heat pumps for provision of hot water or heating/cooling of supply air or both. The heat exchanger consists of a series of pipes buried in shallow ground. The fluid in the heat exchanger can be gas (air) for earth-air tunnel ventilation

(EATV), liquid for a ground source heat pump (GSHP) or a mixture of gas, liquid and solid matters for a wastewater source heat pump. The pipes for an earth-liquid heat exchanger (ELHX) are relatively small, typically 25 mm to 50 mm in diameter [1], and can be installed vertically or horizontally. The pipes for an earth-air heat exchanger (EAHX) are comparatively large, 100 mm or larger, and are generally installed horizontally with a slight inclination to allow condensation to drain away. Drain pipes are used for wastewater heat recovery. This work is focused on the first two types – ELHX and EAHX. For comparison of the thermal performance, the two types of heat exchanger considered here are horizontally installed.

The thermal performance of these heat exchangers has been assessed using experimental, analytical or numerical methods. Mihalakakou, et al. [2] measured hourly air and ground temperatures at various depths below bare and short grass soil at Dublin Airport and revealed that the soil surface cover could be a significant factor for the improvement of the performance of an EAHX. Tiwari, et al. [3] conducted experimental work on a greenhouse with an EAHX for validation of a thermal model in New Delhi. Ozgener and Ozgener [4] measured the performance of a galvanized steel EAHX 47 m long and 0.56 m in diameter for greenhouse cooling in Turkey and found an average cooling coefficient of performance for the system of 10. Gonzalez, et al. [5] measured the interactions between the soil environment and a horizontal slinky heat exchanger for a GSHP in the UK and showed that the heat exchanger modified heat and moisture transport in the soil which in turn could affect the performance of the heat pump. Svec, et al [6] performed a laboratory study of heat flow around plastic pipes buried in clay soil and developed analytical and numerical heat flow models for several configurations. It was shown that the thermal resistance of the pipe wall and the contact resistance at the pipe-soil interface substantially reduced heat flow. Niu, et al [7] developed a one-dimensional steady-state control volume model and results were used to develop a regression model for predicting the sensible, latent and total cooling capacities of an EAHX. Bansal and Mathur [8] developed a thermal model to investigate the potential of an EAHX integrated with an evaporative cooler. The model was derived from an analytical solution of equations for energy, heat transfer and psychrometry to predict the temperature at the outlet of the EAHX. Maerefat and Haghighi [9] also developed a mathematical model based on the energy balance and heat transfer for an integrated system of an EAHX and solar chimney for passive cooling of buildings. Their results indicated that the system performance would depend on the configurations of the solar chimney and EAHX in addition to solar radiation and ambient air temperature.

Analytical techniques such as those mentioned above for ground heat exchangers are generally based on the solution of one-dimensional heat transfer in soil of homogeneous properties. However, heat and moisture transfer occurs simultaneously in moist soil and varies in time and space due to the influence of daily and seasonal climatic variations, inhomogeneous soil composition and its moisture-dependent physical and thermal properties as well as interactions between soil and the heat exchanger. The solution of three-dimensional transport problems requires the use of a numerical method. A numerical model may involve heat transfer only [10-12], or simultaneous heat and moisture transfer but with simplifications [13-14], or heat transfer together with groundwater flow [15]. The present author has developed a more general three-dimensional numerical model for simulation of transient heat and moisture transfer in soil with a horizontally coupled heat exchanger that caters for spatial- and temporal-varying soil properties and includes all the principal interactions of heat and moisture transfer in soil and between atmosphere, soil and the heat exchanger [16]. The model has been used for simulation of dynamic thermal performance of an EAHX for preheating, cooling and ventilation of buildings [17, 18].

This work makes use of the developed numerical model to predict the performance of an ELHX and then compare the performance with an EAHX.

2 Methodology

To simulate the transient thermal performance of a horizontally-coupled ground heat exchanger, a control volume method is used to solve partial differential equations for three-dimensional heat and moisture transfer in soil together with initial and boundary conditions.

The soil for installation of the heat exchanger is assumed to have the following characteristics:

- Dry solid matter in a control volume is homogenous, isotropic and stationary.
- Radiation heat transfer between soil particles is negligible.
- There is no hysteresis between drying and wetting processes.
- External pressure for water movement is absent.
- Effects of solutes are negligible.

The partial differential equations for heat and moisture transfer in such soil can be derived from similar equations for porous materials [19]:

$$\frac{\partial(\rho CT)}{\partial t} = \nabla\left(\left(k + L\rho_l D_{T,v}\right)\nabla T\right) + \nabla\left(L\rho_l D_{\Theta,v}\nabla\Theta\right) + q_v \tag{1}$$

$$\frac{\partial\Theta}{\partial t} = \nabla\left(\left(D_{T,l} + D_{T,v}\right)\nabla T\right) + \nabla\left(\left(D_{\Theta,l} + D_{\Theta,v}\right)\nabla\Theta\right) + \frac{\partial K}{\partial z} + \Theta_v \tag{2}$$

where $D_{T,l}$ and $D_{T,v}$ are the thermal liquid and vapour moisture diffusivities, respectively, (m^2/sK); $D_{\Theta,l}$ and $D_{\Theta,v}$ are the isothermal liquid and vapour moisture diffusivities, respectively, (m^2/s); ρ, C, k and K are the density (kg/m^3), specific heat (J/kgK), thermal conductivity (W/mK) and hydraulic conductivity (m/s) of soil, respectively; L is the latent heat of vaporisation (J/kg); T is the temperature of soil (^{o}C); t is the time (s); z is the vertical coordinate (m); ρ_l is the density of liquid water (kg/m^3); q_v is the volumetric heat production/dissipation rate (W/m^3); Θ is the volumetric moisture content (m^3/m^3); Θ_v is the source/sink of moisture (m^3/m^{3}s).

The four moisture diffusivities and hydraulic conductivity are all dependent on the moisture content of soil whereas the soil density, specific heat and thermal conductivity are functions of the volumetric composition of moisture, dry solid matter and gases [16].

A horizontal heat exchanger is represented by a series of parallel pipes inside a large extended computational domain filled with soil. The boundary of the domain includes the top soil surface, the far-field bottom face and four vertical faces as well as the interior and exterior surfaces of heat exchanger pipes and the inlet and outlet openings for the pipes. Fig. 1 illustrates the boundary conditions on a vertical plane normal to a heat exchanger for preheating and ventilation of a building.

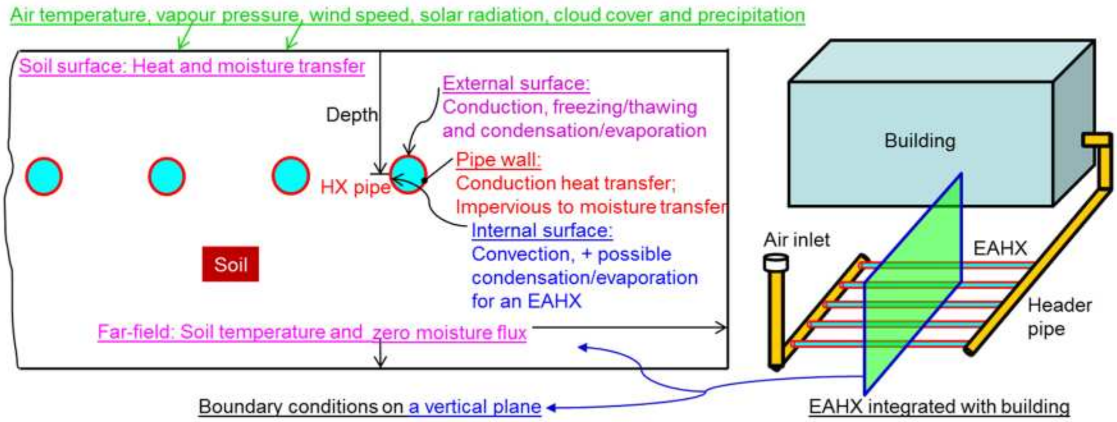

Fig. 1 Boundary conditions for simulation of heat and moisture transfer on a vertical plane normal to the ground heat exchanger

Boundary conditions for the soil surface and the external surface of heat exchanger pipes are derived in a similar form of equations above but for the steady-state and one-dimensional coupled heat and mass transfer because of the interactions between heat and moisture flow.

For heat transfer through the soil surface, applying the total energy balance to a control volume of unit cross section and $\delta\xi$ thickness leads to

$$\left(k + L\rho_l D_{T,v}\right)\frac{\partial T}{\partial \xi} + L\rho_l D_{\Theta,v}\frac{\partial \Theta}{\partial \xi} = \pm q_r \pm q_c \pm q_e \pm q_p \qquad (3)$$

The terms on the right hand side represent the net heat flow due to radiation, convection, evaporation/condensation and precipitation into the control volume and are all dependent on the temperature of soil surface directly or indirectly. The radiation heat transfer (q_r) includes solar radiation and long wave radiation between the soil surface and ambient environment. The hourly solar radiation together with ambient air temperature, vapour pressure, cloud cover and the monthly rainfall is obtained from a local weather station. The long wave radiation is dependent on the soil surface temperature and the sky temperature which is related to the air temperature and cloud cover [16]. The convective heat transfer between the soil surface and ambient air (q_c) results from combined wind and buoyancy effects and is dependent on the soil surface temperature, air temperature, local wind speed and vegetation height [12]. The latent heat transfer due to evaporation of water vapour from the soil surface (or moisture condensation to the soil surface) (q_e) is related to the density and diffusivity of water vapour in air and the temperature and moisture content of the soil surface. The sensible heat transfer due to precipitation (q_p) is associated with the amount of rainfall, soil surface temperature and wet bulb air temperature which is calculated from the temperature and vapour pressure of air [16].

Similarly, the moisture balance at the soil surface results in

$$\left(D_{T,l} + D_{T,v}\right)\frac{\partial T}{\partial \xi} + \left(D_{\Theta,l} + D_{\Theta,v}\right)\frac{\partial \Theta}{\partial \xi} = V_p \pm V_e \tag{4}$$

The terms on the right hand side represent the net flow of moisture due to precipitation (V_p) and evaporation/condensation (V_e).

The solution of Equations (3) and (4), simultaneously with Equations (1) and (2), gives rise to the temperature and moisture content of the soil surface, respectively.

Equations (3) and (4) also apply to the external surface of pipes but with zero values for all the terms on the right hand side.

The calculation of the temperature and moisture level for the internal surface of heat exchanger pipe as the boundary conditions is also based on heat and mass balances. Here heat and mass transfer is dependent on the properties of fluid and the interior surface of pipe, convection heat and mass transfer coefficients. The methodology does not involve detailed calculation of fluid flow inside the heat exchanger. Instead, one-dimensional flow is assumed and the following equation for forced convection [20] is used for calculating heat transfer between the fluid and pipe surface and, by means of heat and mass analogy, analysing moisture transfer between moist air and the pipe surface:

$$h_c = \frac{k_f}{d}\frac{(\mathrm{Re}-1000)\,\mathrm{Pr}}{\left(2.24\ln(\mathrm{Re}) - 4.7\right)\left(2.24\ln(\mathrm{Re}) - 12.7\,\mathrm{Pr}^{2/3} + 8\right)} \tag{5}$$

where h_c is the convective heat transfer coefficient (W/m^2K), k_f is the fluid thermal conductivity (W/mK), d is the internal diameter of the pipe (m), Re is the Reynolds number and Pr is the Prandtl number.

The boundary conditions for heat and moisture transfer at the boundary faces are summarised in Table 1.

Table 1 Boundary conditions for heat and moisture transfer

Type of boundary	Heat transfer		Moisture transfer	
Top soil surface	Equation (3)		Equation (4)	
Outer pipe surface	Equation (3) with zero heat flux on the right hand side		Equation (4) with zero mass flux on the right hand side	
Far-field	Equation (6)		Zero mass flux	
Pipe outlet	Zero heat flux		Zero mass flux	
Pipe fluid	*Air*	*Refrigerant*	*Air*	*Refrigerant*
Pipe inlet	Ambient air temperature (varying with time) and flow rate (or velocity)	Temperature (varying with time) and flow rate (or velocity)	Vapour pressure (varying with time)	100% liquid
	Zero heat and mass flux when heat extraction not feasible			
Inner pipe surface	Convection (Equation (5)) + Condensation (evaporation)	Convection (Equation (5))	Condensation (evaporation)	Zero mass flux

The initial soil moisture content is assumed to be uniform whereas the initial soil temperature profile is taken to be the following expression for the annual variation of the soil temperature at depth Z (m) at the start of system operation

$$T = T_m - T_{amp} e^{-Z/D} \sin\left((t_d - t_{dl}) \frac{2\pi}{365} - \frac{Z}{D} - \frac{\pi}{2} \right) \tag{6}$$

where T_m is the annual mean temperature of deep soil (°C), T_{amp} is the annual amplitude of surface temperature (°C), t_d is the time in day and t_{dl} is the time lag from a starting date to the occurrence of the minimum temperature in a year and D is the damping depth (m) of annual fluctuation defined as

$$D = \sqrt{\frac{365}{\pi} \frac{86400k}{\rho C}} \tag{7}$$

Equations (1) and (2) are solved using the control volume method. For spatial descretisation, a three-dimensional computational domain is first divided into small control volumes or cells. Each equation is then integrated spatially over each cell to obtain an integral equation. Next, the integral equation is discretised into an algebraic equation. As the equations do not involve terms representing fluid flow by convection, spatial discretisation of a diffusion term at a cell is along two neighboring cells in each direction. Finally, all the algebraic equations are solved iteratively for all cells at each time. For temporal discretisation, the forward Euler method is used. Both cell and time step sizes vary in space and time, respectively, in order to ensure solution stability while achieving accurate solution as well as solution independency of the sizes. Fine cells are concentrated near the boundary with atmosphere and the heat exchanger where variations of heat and moisture transfer are large. The smallest edge size is about 1 mm and the cell size increases gradually from the boundary [17]. Likewise, small time steps are used when large variations in heat and moisture transfer occur. These include the times at the beginning of system operation, when the system is switched on or off for intermittent operation and similarly for the switch-off and -on period when heat extraction/injection is not feasible due to the higher fluid temperature than that of surrounding soil in heating operation or lower fluid temperature in cooling operation. The time step increases gradually from one second for the first hour to one minute, two and five minutes after continuously heating/cooling for 12 hours, two days and 10 days, respectively. A flow chart for the prediction of heat and moisture transfer in soil is shown in Fig. 2.

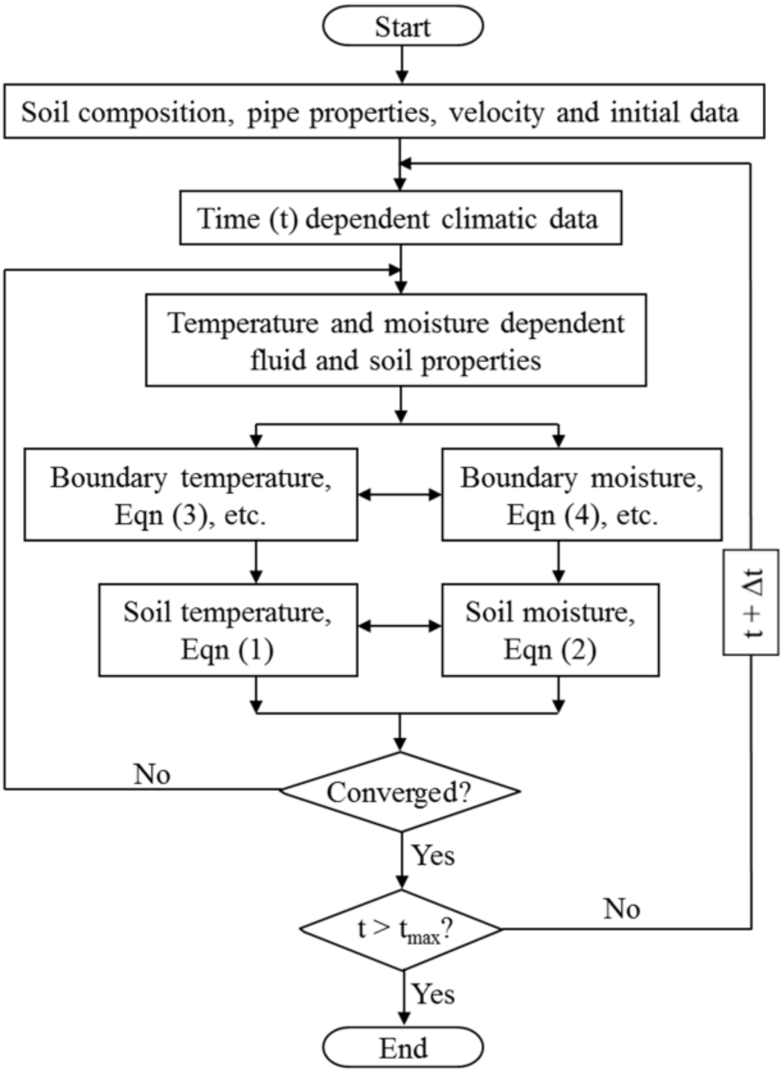

Fig. 2 Flow chart for the prediction of heat and moisture transfer in soil

The model has been validated for simulation of transient heat transfer in soil for heat extraction through an EAHX of 200 mm external diameter buried 1.5 m below the ground with an initial deep soil temperature of 10°C in the Southern England and under constant environmental conditions [16, 17]. To ascertain the accuracy of the in-house program for the model, further validation is carried out through comparison of results with commercial software FLUENT [21]. Use is made of the soil properties measured from the same site - soil density, specific heat and thermal conductivity of 1588 kg/m^3, 1465 J/kgK and 1.24 W/mK, respectively [11]. Time-dependent environmental conditions (air temperature, wind speed and associated heat transfer coefficient) are used for October at the same installation site described in the next section where the daily air temperature varies by over 6°C, daily wind speed varies from 1.8 m/s to 4.1 m/s and soil temperature at 1.5 m deep is about 14°C at the beginning of the month. The fluid (i.e., air) temperature in the pipe is however fixed at 1°C instead of varying with ambient. As a result, the convective heat transfer coefficient for the soil surface due to both buoyancy and wind effects varies with time but the coefficient for forced convection inside the pipe is constant at 8.7 W/m^{2}K based on Equation (5) for an air velocity of 2 m/s and temperature of 1°C. The deep soil temperature for the site is about 10°C and this is also used as the initial soil temperature. In order to compare the results from the two programs, firstly, transient heat transfer simulation is carried out using the in-house program with optimised time steps [16], which gives rise to not only varying heat transfer rate through the heat exchanger with time but also varying heat transfer coefficient at the soil surface. The same values of boundary conditions and time steps are then used in FLUENT for simulation of transient conduction heat transfer through the same soil-pipe configuration without involvement of any fluid flow equations. Fig. 3 shows that the predicted heat transfer rate using the in-house and FLUENT programs for a period of 10 days. It is seen that the predicted heat transfer rates between the two programs agree very well.

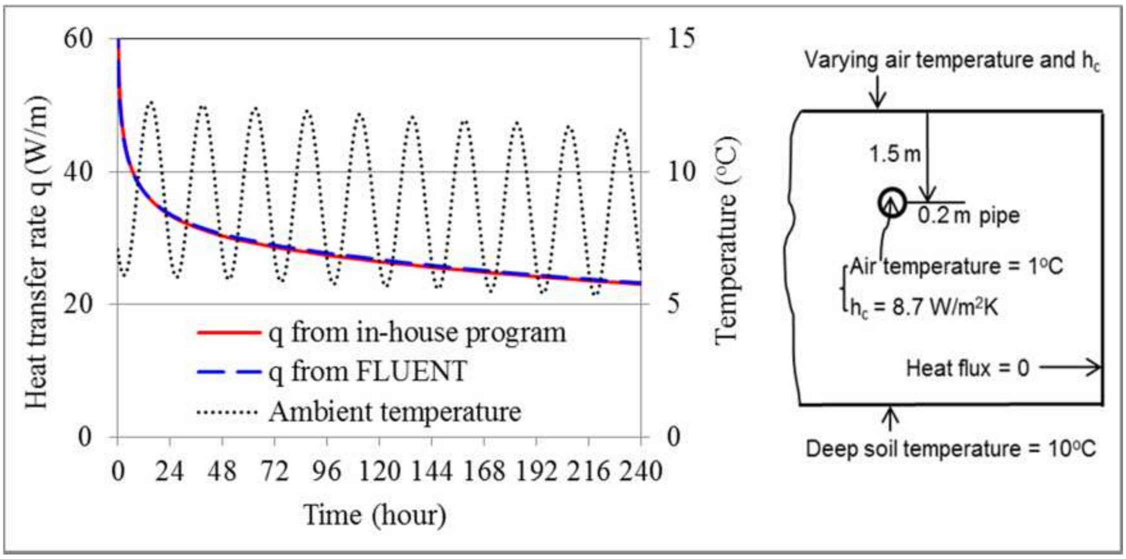

Fig. 3 Comparison of the predicted heat transfer rate between the in-house and FLUENT programs

3 Results and discussion

The numerical method is next applied to assessing the performance of an ELHX for a ground source heat pump and an EAHX for preheating of supply air for buildings under climatic conditions in the Southern England. Both heat exchangers are made of high density polyethylene and installed horizontally at 1.5 m below the ground surface. Table 2 shows the dimensions of the heat exchangers and fluid properties and Table 3 shows the properties of soil in consideration. The pipe sizes and inlet fluid velocities for simulation are not the same but are typical values for operating the two different types of system [1, 22]. Even though the air velocity in a larger pipe is much higher, the mass flow rate through the liquid pipe is about five times higher than that in the air pipe. For a start, the temperature of incoming fluid is set the same as varying ambient air temperature for both types of heat exchanger, in addition to varying meteorological data including air temperature, vapour pressure, solar radiation, cloud cover and wind speed [23] as well as rainfall [24]. The effects of soil temperature and moisture, and the thermal resistance of pipe wall are then investigated. Later on, simulation is also carried out for more practical conditions with the liquid temperature independent of the ambient temperature. In addition, the performance is compared for the two heat exchangers operating with the same mass flow rate. Comparison is also made using the two-dimensional and three-dimensional models for an ELHX. A summary of the simulation cases is given in Table 4.

Table 2 Properties of heat exchangers and fluids

Type of heat exchanger	EAHX [22]	ELHX [1]
External diameter (mm)	200	40
Internal diameter (mm)	184.6	32.6
Fluid	Air	65% water and 35% antifreeze
Inlet velocity (m/s)	2	0.4
Reynolds number (at starting conditions)	27015	3494

Table 3 Properties of soil [25]

Type		Loamy
Composition		43% sand, 18% clay and 39% silt
Moisture content (%)	Saturation	44
	Residual	5
	Initial	22
Temperature of deep soil (^oC)		10

Table 4 Summary of simulation cases

Type of heat exchanger	Soil temperature	Soil moisture	Incoming fluid	Pipe material	Discussed in section
ELHX	Dynamically variable	Dynamically variable	Variable properties	Plastic	3.1.1
ELHX	Equation (6)	Constant at 0.22 m^3/m^3	Variable properties	Plastic	3.1.2
ELHX	Equation (6)	Constant at 0.3 m^3/m^3	Variable properties	Plastic	3.1.2
ELHX	Dynamically variable	Dynamically variable	Variable properties	Metal	3.1.2
ELHX	Equation (6)	Constant at 0.22 m^3/m^3	Variable properties	Metal	3.1.2
EAHX	Dynamically variable	Dynamically variable	Variable properties	Plastic	3.2
EAHX	Equation (6)	Constant at 0.22 m^3/m^3	Variable properties	Plastic	3.2
EAHX	Dynamically variable	Dynamically variable	Variable properties	Metal	3.2
ELHX	Dynamically variable	Dynamically variable	Monthly mean air temperature	Plastic	3.3
ELHX	Dynamically variable	Dynamically variable	Daily mean air temperature	Plastic	3.3
ELHX	Dynamically variable	Dynamically variable	Variable properties; <u>intermittent operation</u>	Plastic	3.3
EAHX	Dynamically variable	Dynamically variable	Variable properties; <u>same mass flow rate as for ELHX</u>	Plastic	3.4
ELHX	Dynamically variable; <u>2D model</u>	Dynamically variable; <u>2D model</u>	Variable properties	Plastic	3.5

Results are first discussed for the ELHX and then compared with the EAHX.

3.1 Earth-liquid heat exchanger

The general trend of variation of heat transfer through a heat exchanger is dependent on the soil and atmospheric conditions. The air temperature at the site varies by about 5°C at the beginning of January to 6.6°C at the end of the month. The daily variation in the temperature of the undisturbed soil at 1.5 m deep is negligible but change occurs gradually during the month, decreasing from about 8^{o}C at the beginning of the month to 6.2^{o}C at the end of the month, in contrast with increasing air temperature (illustrated in Fig. 6a for three months for reference). The undisturbed soil temperature is higher than the night time air temperature throughout the month but near the end of the month the air temperature for a short period of daytime could rise above the soil temperature, implying that heat could not be transferred from the soil when operating with a fluid at the same temperature as ambient air such as the EAHX.

3.1.1 Variations of heat transfer

Heat transfer through a heat exchanger varies with time and space (along the axis and circumference). The heat transfer rate between the heat exchanger and the fluid within varies along the heat exchanger and in the absence of condensation/evaporation during heat extraction the heat transfer rate per unit length of the heat exchanger (q in W/m), or specific heat extraction, is obtained from the following equation:

$$q = \pi d \frac{\sum h_c (T_p - T_f)\Delta x}{l} \tag{8}$$

where l is the pipe length (m), T_s is the temperature of the interior surface of the pipe (^{o}C) and T_f is the fluid temperature (^{o}C), at section Δx.

The amount of daily heat transfer (i.e., energy, E in Wh/m) is the cumulative product of the heat transfer rate and time step (Δt) for the duration of heating period, ie.

$$E = \frac{\sum q\Delta t}{3600} \tag{9}$$

Fig. 4 shows the predicted variation with time in the amount and rate of heat transfer per unit length of a 10 m long heat exchanger in January. The heat transfer rate depends on soil and ambient temperatures. Because the soil temperature is more stable than air temperature, the heat transfer rate is higher during the night when the air temperature (= inlet fluid temperature) is much lower than that in the daytime and this is shown in Fig 4a for the first five days of the month. It generally peaks at about 2am and decreases for a period of 12 hours to a minimum at about 2pm and then increases for 12 hours. For the first day, however, the heat transfer rate peaks at the beginning (midnight) as the heat exchanger is assumed to be at equilibrium with surrounding soil and the cold fluid from the inlet flows forward slowly - it takes 25 seconds for the cold fluid to travel at 0.4 m/s through the 10 m long heat exchanger. In terms of variation between operating days, Fig. 4b shows that the heat transfer rate would decrease due to decreasing soil temperature and from Day 4 the minimum value drops to zero at about 1pm when the ambient air temperature becomes higher than the temperature of the soil at the pipe inlet. Subsequently, heat in surrounding soil would not be available for extraction and preheating of supply fluid in the heat exchanger is supposed to stop. The duration when heat extraction is not feasible increases with operating time from two hours (1pm to 3pm) on Day 4 to 12 hours on the last day of the month from 8am to 8pm, i.e., no preheating potential during the daytime.

As heat could not be extracted all day long from Day 4, the daily heat transfer decreases faster than does the heat transfer rate as shown in Fig. 4b. Taking mean values for Day 5 and Day 30 as examples, the peak heat transfer rate (at 2am) decreases by 19% from 19.1 to 15.5 W/m, respectively, while the daily heat transfer decreases by 45% from 219 to 120 Wh/m, for a 10 m long heat exchanger.

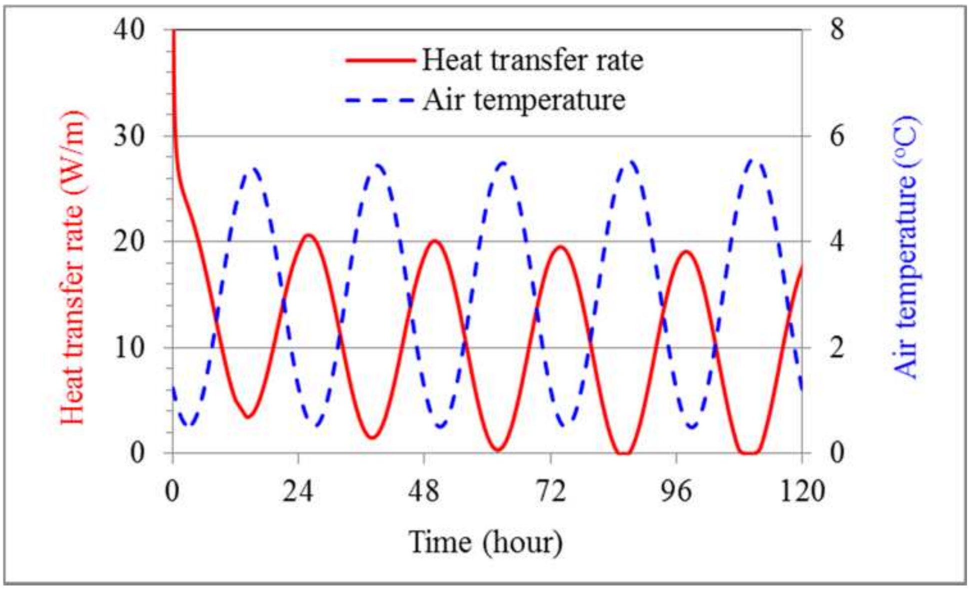

(a) Heat transfer rate and air temperature for five days

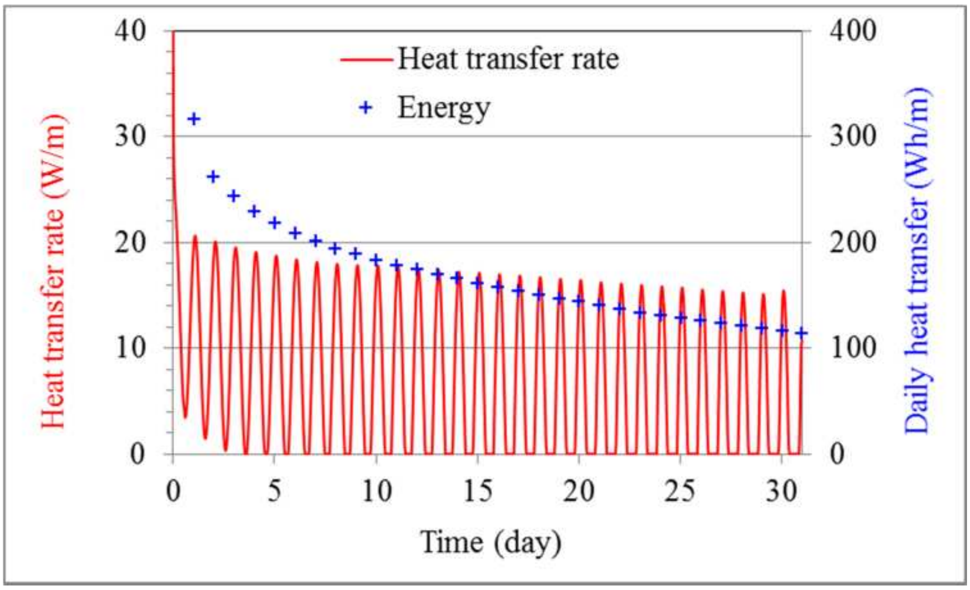

(b) Heat transfer for the month

Fig. 4 Predicted variation in the heat transfer through a 10 m long ELHX in January

In general, because of the increase in the fluid temperature and the decrease in the temperature difference along the flow passage, heat transfer decreases along the flow direction in the heat exchanger. This leads to the decrease of the length-averaged mean heat transfer with increasing length of the heat exchanger. However, due to the high mass flow rate, the temperature increase in the liquid pipe is not significant; it is less than 0.2^{o}C and 1^{o}C through 10 m and 40 m long heat exchangers, respectively, after flow is fully established. Fig. 5 shows that the daily heat transfer is similar for 10 m and 40 m long heat exchangers in January. The length-averaged heat transfer through the 10 m long heat exchanger is at most only 3% higher than that for the 40 m long heat exchanger. Hence, the specific heat extraction for a ground source heat pump can be considered nearly independent of the length of the ground heat exchanger. In other words, computationally a two-dimensional model may be used for evaluation of three-dimensional heat and liquid flow through straight pipes with a maximum error of 1% per 10 m length increase for typical operating conditions. This will be explored further later on.

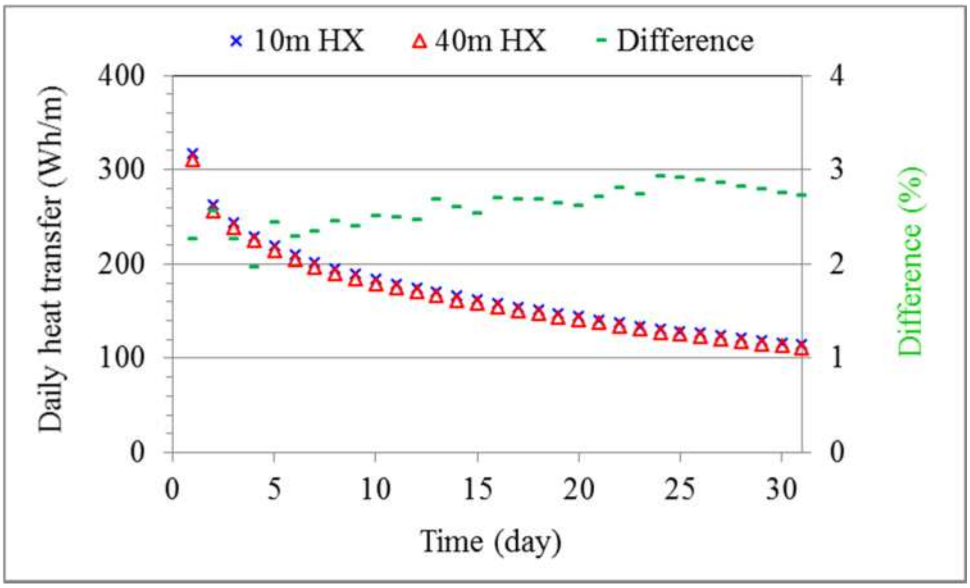

Fig. 5 Predicted daily heat transfer through 10 m and 40 m long ELHXs in January

3.1.2 Effect of interactions between the heat exchanger, soil and atmosphere

Because of heat extraction, the temperature of soil surrounding the heat exchanger becomes much lower than that of the undisturbed soil at the same depth and this ultimately limits the rate and extent of available heat for extraction. Meanwhile heat and moisture transfer in shallow ground is influenced by ever changing atmospheric conditions. Hence, heat transfer through the heat exchanger is highly influenced by the interactions between the fluid and surrounding soil and between soil and atmosphere. Without consideration of these interactions, heat transfer could not be calculated accurately. For example, using Equation (6) to calculate the soil temperature at pipe location ignores the interactions between the heat exchanger and surrounding soil. Fig. 6 shows the effect of the interactions on the predicted heat transfer for three months from January to March. In order to show variations clearly, only the daily minimum and maximum values are presented in Fig. 6a for the heat transfer rate and ambient air temperature. The predicted heat transfer without considering the interactions is much higher in January and February. The predicted daily variation results mainly from assumed variation in the fluid temperature and, because the calculated soil temperature remains high and stable while the fluid temperature varies considerably, the daily heat transfer variation is also much larger than that when the influence of varying soil temperature is taken into consideration. The higher heat transfer rate in combination with a longer period for potential heat extraction each day – continuous for 21 days compared with three days only with consideration of the interactions – leads to a larger difference in the amount of daily heat extraction predicted with and without consideration of the interactions than that in the heat transfer rate in January and February. Without considering the interactions, the amount of daily heat transfer would considerably be over predicted and the over-prediction would increase with operating time up to the 11th day when the over-prediction reaches 463% for a 10 m long heat exchanger.

Another noticeable feature observed from Fig. 6 is that after a few days' operation both the rate and amount of heat transfer decrease faster with time on a daily basis when the interactions are ignored. For example, the daily heat transfer decreases by 48% from 1033 Wh/m on Day 10 to 539 Wh/m on the last day of January without considering the interactions whereas the corresponding decrease is 38% from 184 Wh/m to 114 Wh/m with consideration of the interactions. This is because the interactions result in less heat available for extraction from soil surrounding the heat exchanger each day and consequently less daily variation with time. Thus, the difference between with and without consideration of the interactions would decrease with increasing operating time. On Day 79, the predicted daily heat transfer is almost the same from the two methods. From Day 80 (in later March), the predicted heat transfer with consideration of interactions would become higher than that without considering the interactions because the predicted temperature of soil surrounding the heat exchanger is still higher than the ambient air temperature from the midnight for five to six hours. However, the soil temperature calculated from Equation (6), though increasing with time, is higher than the ambient temperature by only a fraction of degree for one hour or so at the end of March.

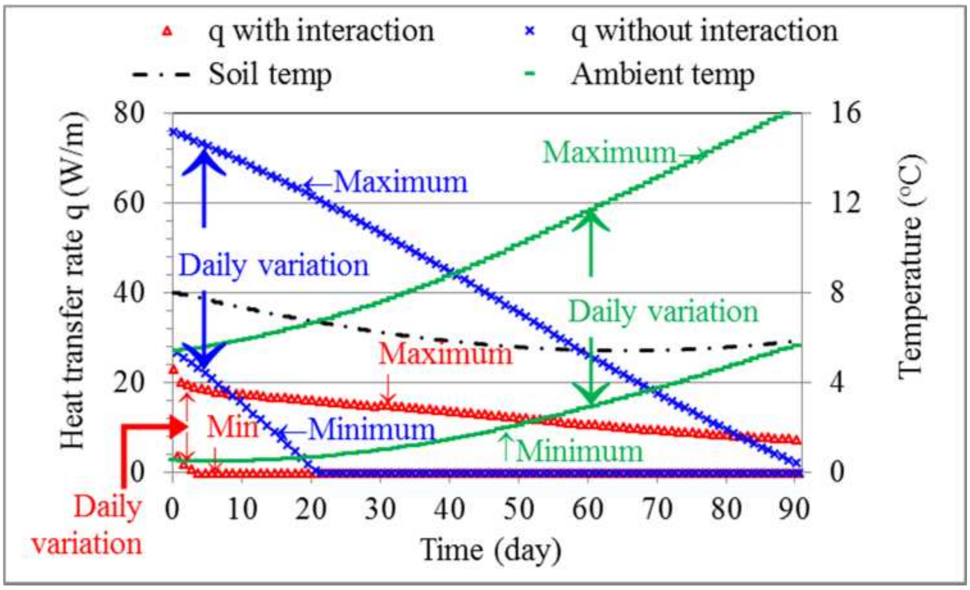

(b) Minimum and maximum heat transfer rate

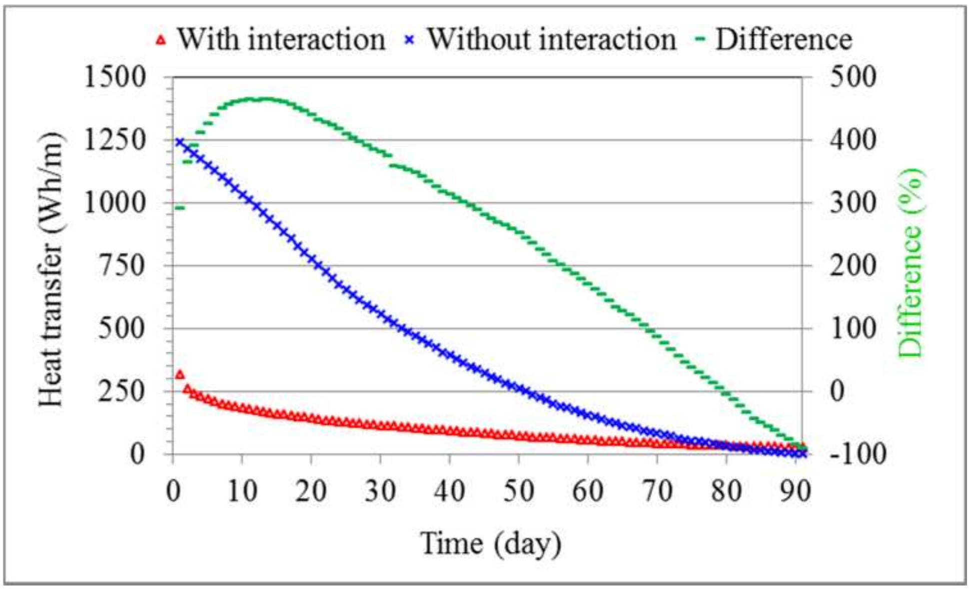

(b) Daily heat transfer

Fig. 6 Effect of interactions on the predicted heat transfer for a 10 m long ELHX from January to March

A major problem with analytic expressions for the annual soil temperature profile such as Equation (6) is the assumption of constant and uniform soil properties, in addition to their inability to account for the influence of the heat exchanger or similar devices. The damping depth in Equation (6), D, depends on the thermal properties which are neither constant nor uniform in shallow ground [16] due to varying soil moisture content as an example. The calculated soil temperature at the installation depth so far is based on the thermal properties with a moisture content of 0.22 m^3/m^3, i.e. approximately one half of the saturation level as an annual average. The soil moisture content at the end of March is about 0.3 m^3/m^3 from the simulation using

Equations (1) and (2). The resulting daily heat transfer based on Equation (6) with soil properties at a moisture content of 0.22 and 0.3 m^3/m^3 is 2.29 and 3.07 Wh/m, respectively, for the last day of March. Hence, the calculated heat extraction would increase by about 1/3 with increased soil moisture. This large increase is however relative to the marginal amount of heat available for extraction on the day. The increase for more heat extraction would be smaller - around 3% to 6% when the daily heat transfer is larger than 40 Wh/m and up to 10% when the daily heat transfer decreases to 20 Wh/m.

It has also been found that the thermal resistance of the heat exchanger, which has a lower thermal diffusivity (2.7×10^{-7} m^2/s) than unsaturated soil (6.1×10^{-7} m^2/s at 0.3 m^3/m^3 moisture content), plays a significant role in (limiting) heat extraction. The calculated specific heat extraction based on Equation (6) would be increased by over 80% when the thermal properties of the heat exchanger were set the same as those for soil, which would be similar to a case with thin metal pipes with the same internal diameter whose thermal resistance is negligible compared with soil while the volume of the shell for the original plastic pipes was mostly displaced with soil. For instance, the specific heat extraction would be increased to 2198 and 1829 Wh/m for the 2nd and 11th day of January, respectively, and 5.5 Wh/m for the last day of March. Such a seemingly large influence of the thermal properties of the heat exchanger is the consequence of neglecting the thermal resistance of surrounding soil in Equation (6). By comparison, the soil thermal resistance is included when consideration is given to the full interactions between the soil and surrounding environments using Equations (1) and (2). Thus, when the heat exchanger and soil were assumed to have the same thermal properties, the increase in the predicted heat transfer would be about 10% to 12%. The influence of the thermal resistance of the heat exchanger on heat transfer is consistent with the laboratory measurement by Svec, et al [6].

A peculiar phenomenon has been observed from the dynamic interactions with the environments: the heat transfer rate through a ground heat exchanger with a larger thermal resistance could be higher than that with a smaller resistance for several hours during the daytime. Fig. 7 shows a comparison of the heat transfer rate for two heat exchangers – one for the original plastic pipes (denoted as q for large resistance) and the other for the heat exchanger with the same thermal properties as surrounding soil (q for small resistance), together with the fluid temperature (= ambient temperature) for the second day of January. It is seen that heat transfer rate is generally higher when the heat exchanger is set with the same thermal properties as surrounding soil. However, during the daytime between 9am and 4pm, the heat transfer rate through the plastic heat exchanger would be slightly higher. The reason for this phenomenon is that for the heat exchanger with a smaller resistance, the soil temperature decreases faster during the night and early morning when the fluid temperature is low such that from around 9am the product of the overall heat transfer coefficient for the heat exchanger and the temperature difference between the surrounding soil and fluid becomes lower than that for the heat exchanger with a larger resistance. In fact, heat would not be available for extraction during 1pm to 3pm on the 2nd day of the month using the heat exchanger with the small resistance instead of the 4th day using the plastic pipes. After the fluid temperature peaks at about 3pm, the heat transfer rate through the heat exchanger with a smaller resistance soon turns higher. This unusual phenomenon would not occur for heat transfer at a constant fluid temperature, as dictated by the heat balance equation.

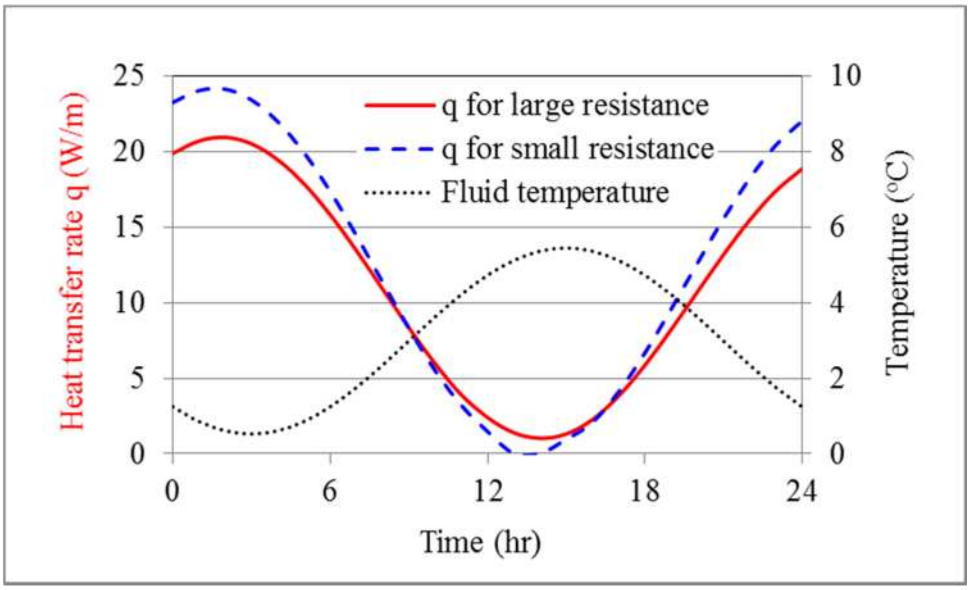

Fig. 7 Effect of thermal resistance of heat exchanger on the predicted heat transfer

3.2 Comparison between two types of heat exchanger

Figure 8 shows a comparison of the amount of daily heat transfer per unit length of 10 m long EAHX for EATV and ELHX for GSHP in January. The amount of heat transfer through the ELHX is larger than that for the EAHX because of the larger mass flow rate of the liquid so that the heat transfer rate and fluid temperature are nearly constant along the liquid pipe whereas the heat transfer rate decreases considerably along the air pipe due to increasing air temperature. For 10 m long heat exchangers, the difference in the daily heat transfer is around 11% in the early days (from the 2nd to 4th day) and increases to about 27% at the end of the month. The increasing difference with time is the result of decreasing heating potential – higher mean fluid temperature in the air pipe than that in the liquid pipe.

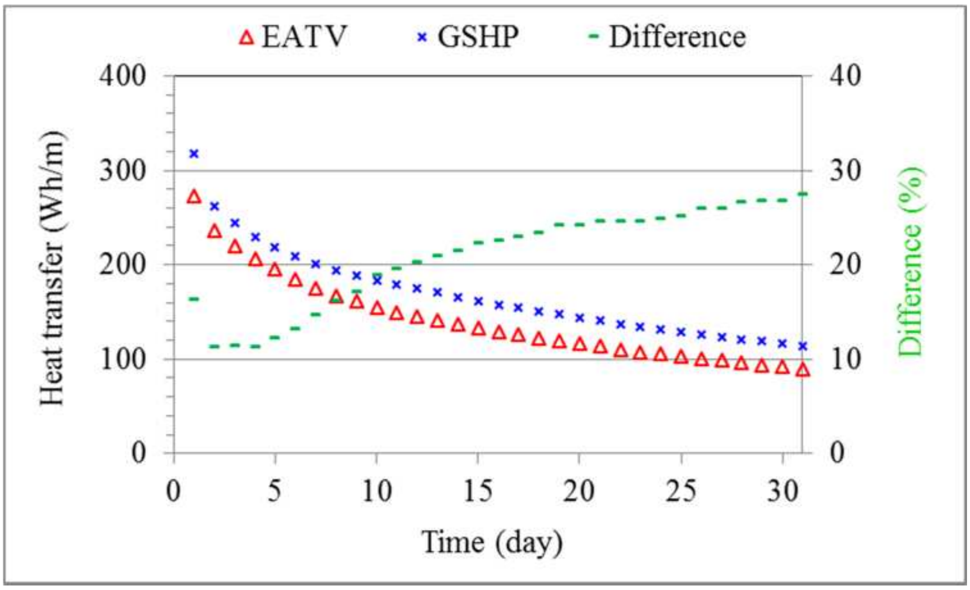

Fig. 8 Predicted variation of daily heat transfer for two types of heat exchanger 10 m long in January

The length-averaged mean heat transfer decreases with the increase in the length of heat exchanger and the rate of decrease is directly linked to the increase of the fluid temperature in the heat exchanger. As the mass flow rate in the air pipe is much lower, the temperature increase and heat transfer decrease in the air pipe are much larger than those in the liquid pipe. For example, the air temperature increase through a 40 m long heat exchanger could be as much as 6^{o}C whereas the liquid temperature increase would be no more than 1^{o}C. Consequently, the difference in mean heat transfer between the liquid and air pipes increases with the length of heat exchanger almost linearly as shown in Fig. 9. By contrast, the heat transfer decreases along the heat exchanger as mentioned above and the decrease in an EAHX is quite non-linear [17]. Also, heat transfer in the air pipe decreases faster with time than that in the liquid pipe so that the relative difference generally increases with operating time. An exception is near the beginning of operation when the heat transfer difference is quite large under the same soil and atmospheric conditions. The difference increases from 11% for a 10 m long pipe to 68% for a 40 m long pipe in the early days (the 2nd to 4th day), respectively, and from 27% for a 10 m long pipe to 89% for a 40 m long pipe at the end of the month.

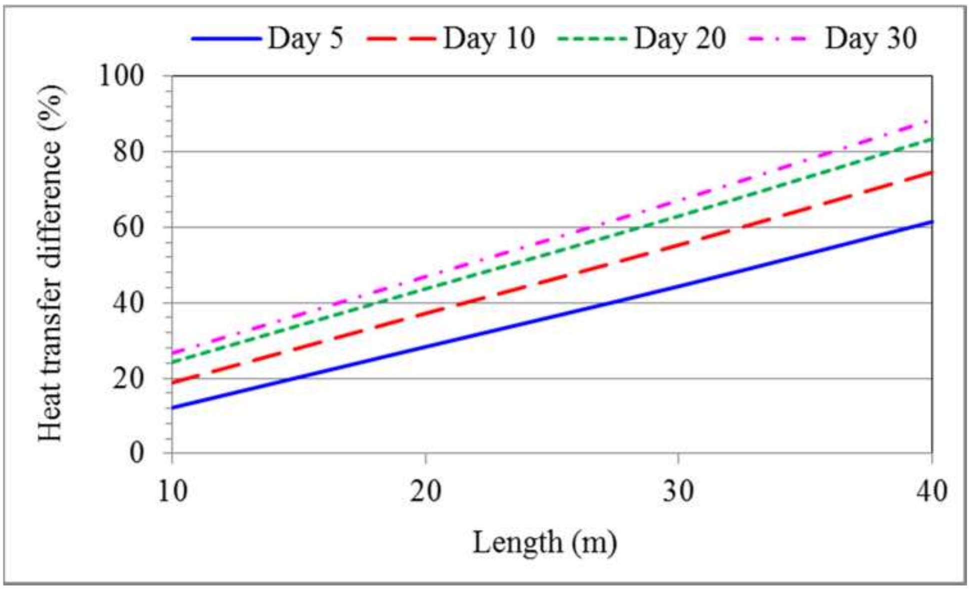

(a) For selected days

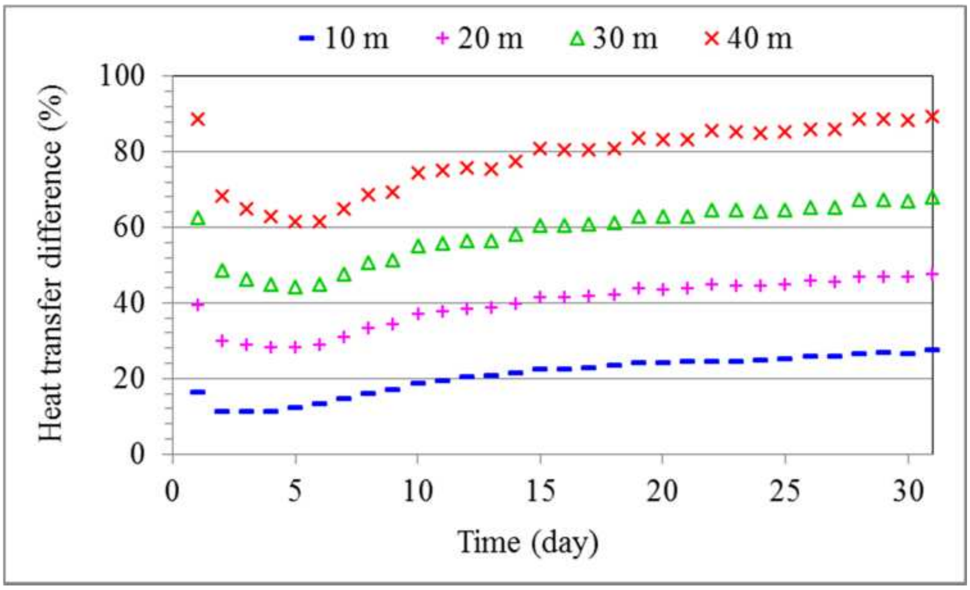

(b) For selected lengths

Fig. 9 Difference in the predicted daily heat transfer through two types of heat exchanger in January

The effect of the interactions between the heat exchanger and soil for an EAHX is smaller than that for an ELHX. This is because the smaller mass flow rate in the EAHX results in smaller heat transfer rate and soil temperature decrease. Nevertheless the difference in the predicted heat transfer could still be substantial; the maximum difference in the daily heat extraction reaches 112% for a 10 m long earth-air pipe [17], compared with 463% for the earth-liquid pipe. The effect of the interactions for both types of ground heat exchanger would have significant implications for system design and performance evaluation. A dynamic simulation would be required to provide accurate data for design or analysis. It is well known that there is a large gap between designed and in-use performance of buildings in terms of energy use. For a building designed with such a GSHP or EATV system based on a method that neglects the dynamic interactions between the heat exchanger and surrounding environments, the in-use energy performance would be worse than designed.

Besides, the effect of thermal resistance of an EAHX is much smaller than that of an ELHX because the film resistance of the internal surface of the EAHX is much larger than the thermal resistance of the pipe wall. When the pipe properties for the EAHX were replaced with those of soil, the increase in heat transfer was between 2% and 4% compared with 10% - 12% for the ELHX.

3.3 Comparison between varying and constant fluid temperatures

In practice, the temperature of the fluid in a heat exchanger for a ground source heat pump does not follow or vary as much as that of ambient air. To compare with the results using the varying fluid temperature, prediction was also carried out for a constant fluid temperature of 3.3ºC (the monthly mean ambient air temperature in January).

Figure 10a shows that the instantaneous heat transfer rate differs significantly using constant and varying temperatures. The heat transfer rate is nearly constant throughout a day when the incoming fluid temperature is fixed. The heat transfer rate using a fixed fluid temperature of 3.3ºC is much lower than the peak value (at night time) predicted with varying fluid temperatures. It is only about 1/3 of the peak near the end of the month. However, because heat could not be extracted all day long when the incoming fluid temperature is the same as the ambient air temperature whereas heat could be extracted continuously using a constant incoming fluid temperature (lower than the surrounding soil temperature), the predicted amount of daily heat transfer using the two different types of temperature setting is similar as shown in Fig. 10b. The maximum difference using two different temperatures is less than 9% for the whole month. The overall trend in the difference between the two is that the higher heat transfer predicted with the varying fluid temperature at the beginning gradually becomes lower as heating operation proceeds. The reason for this trend is that the daily mean ambient air temperature gradually increases with time rather than constant. This would suggest that if the incoming fluid temperature was set as the daily mean air temperature, the difference between the two might have been smaller. However, it turns out that such daily mean values can only be used for prediction for short-term operation but would not be suitable for long-term continuous operation. This is because the predicted heat available for extraction using the increasing daily mean temperature (i.e., decreasing temperature difference between soil and fluid) decreases faster than using continuously varying fluid temperature. Fig. 10b also shows that the predicted heat transfer using the daily mean temperature is quite close to that using the varying temperature for the first week's operation, with a maximum difference of less than 2%. Compared with the prediction using the varying fluid temperature, the difference using the daily mean temperature is smaller than that using the monthly mean temperature for 13 days' operation but becomes larger afterwards. For example, the predicted difference in the daily heat transfer for the first day is reduced from just under 6% using the monthly mean air temperature (3.3°C) to within 1% using the daily mean temperature of 3°C and for the 10th day reduced from 7% to 5% using the daily mean temperature of 3.2°C. However, on the 15th, 20th and 31st days, the predicted daily heat transfer using the corresponding daily mean temperatures would be 11%, 20% and 44%, respectively, less than that using the varying fluid temperature.

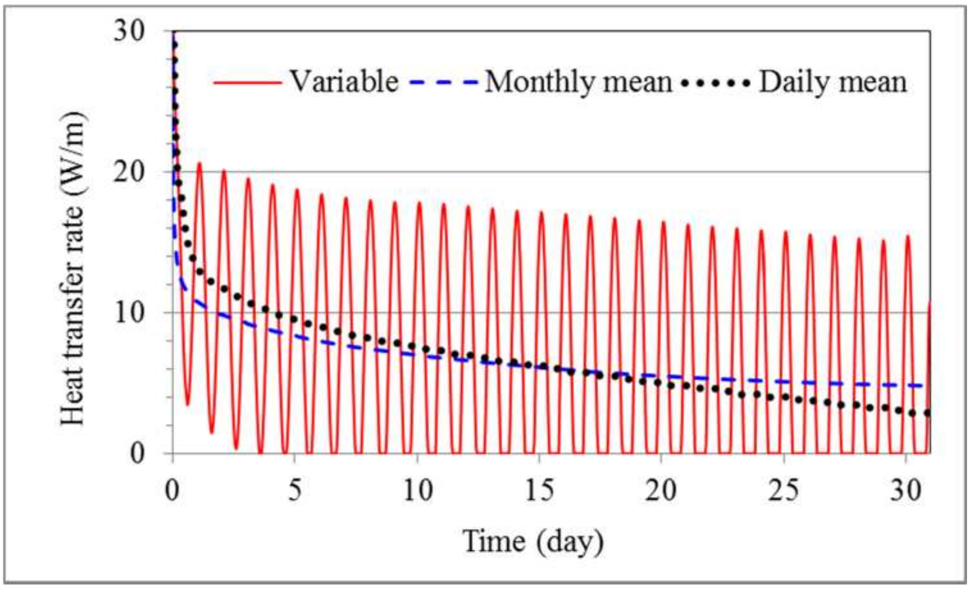

(a) Instantaneous heat transfer rate

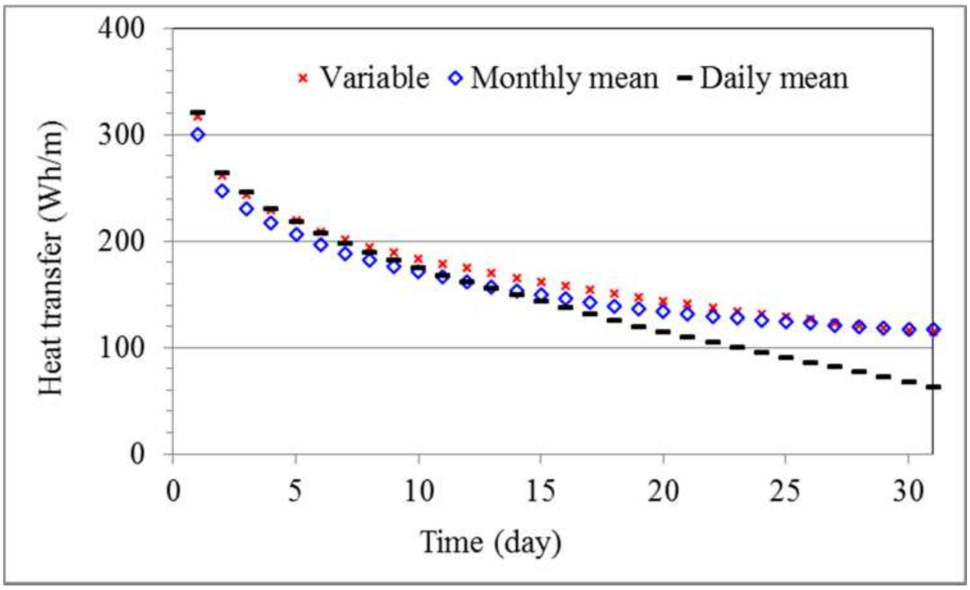

(b) Daily heat transfer

Fig. 10 Predicted daily heat transfer through an ELHX with monthly mean, daily mean and varying incoming fluid temperatures in January

The predicted amount of daily heat transfer is similar using constant (monthly mean) and varying fluid temperatures but this is only true for continuous operation for a period of a day when heat is available for extraction using the varying fluid temperature in comparison with all the time using the constant temperature. Because the instantaneous heat transfer rate differs significantly, the predicted amount of daily heat transfer could differ too using two different temperatures for intermittent operation when the mean ambient air temperature for the operating period differs from the monthly mean value. Fig. 11 shows that the predicted heat transfer using a constant temperature could be much higher or lower than that using the varying temperature for intermittent operation between 8am and 8pm, depending on the period for taking the mean temperature. The mean air temperature for the 12-hour daytime operating period is higher than that for the night time. Hence, using the (12 hour) night time mean air temperature would give rise to much higher heat transfer and using the (12 hour) daytime mean air temperature would lead to much lower heat transfer – negligible heat extraction from Day 21.

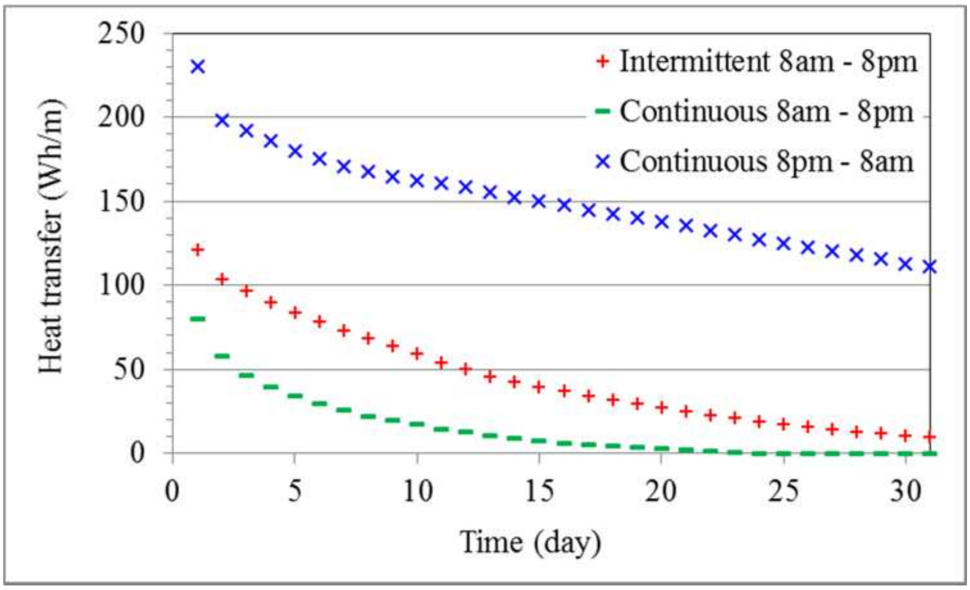

Fig. 11 Comparison of predicted daily heat transfer through an ELHX for intermittent and continuous operation in January

3.4 Comparison for the same mass flow rate

The above comparisons between two types of heat exchanger are based on their typical design and operating conditions. A further simulation is performed for an EAHX with the pipe size increased to 0.315 m in external diameter and incoming velocity to about 4.1 m/s such that the mass flow rate is the same as that for the ELHX. It should be pointed out that comparison could also be made for the same original pipe of 0.2 m in diameter but the fluid velocity would be excessive (> 10 m/s). Fig. 12 shows that the predicted heat transfer per unit length of the EAHX is higher than that of the ELHX at the same flow rate. The difference is 42% at the beginning and decreases to around 28% on Day 13 and onwards. However, in terms of heat transfer per unit pipe surface area, i.e. heat or energy flux, the smaller ELHX is still more effective with the heat flux over four to five times higher than that for the larger EAHX because of the much larger heat transfer coefficient.

One implication from this comparison is that a GSHP is more efficient for heating or cooling of supply air than an EATV system if preheated or cooled air needs to be further enhanced with supplementary heating/cooling using electricity, e.g., through an air source heat pump.

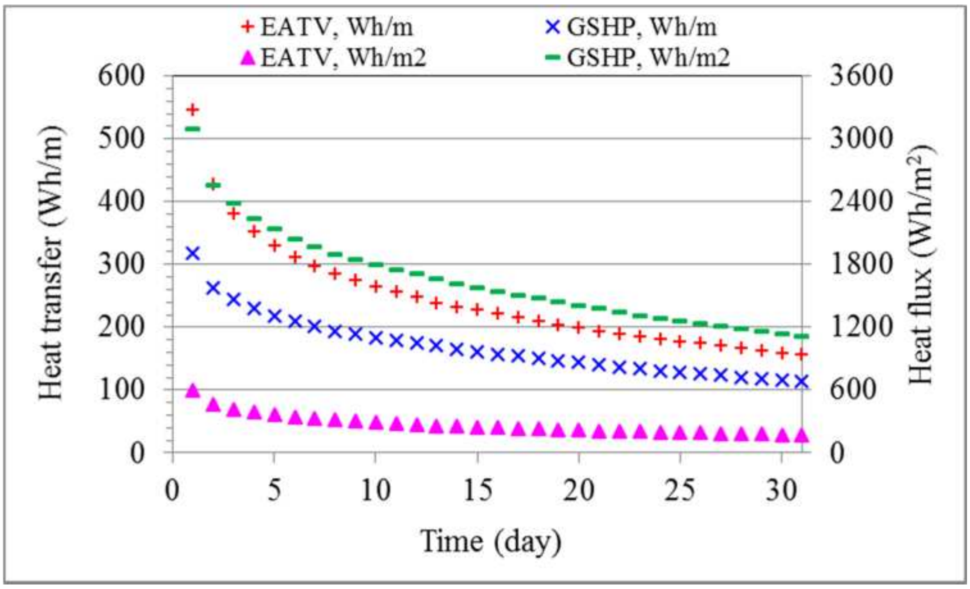

Fig. 12 Predicted variation of daily heat transfer for two types of 10 m long heat exchanger at the same mass flow rate

3.5 Comparison between two- and three-dimensional models

As pointed out earlier, temperature and heat transfer variations along the flow passage of an ELHX are negligible, suggesting a possibility for simplifying the three-dimensional model into a two-dimensional model normal to the flow passage. However, the difference or the error from the simplification could depend on the operating time. If the difference between the two- and three-dimensional models increases with operating time, it could become significant for long term operation.

To assess the effect of the simplification, a two-dimensional model is also used for simulation. The two-dimensional model is based on an equivalent unit size in the fluid flow direction and hence the results are independent of the length of heat exchanger. On the other hand, results from the three-dimensional model have shown that the fluid temperature increases and the heating potential decreases along the flow passage for heating operation. Fig. 13 show the difference of the predicted daily heat transfer results between three-dimensional and two-dimensional models. In general, a two-dimensional model would under-predict the performance for short heat exchangers (positive difference in Fig. 13) and over-predict it for long heat exchangers (negative difference in the figure). The difference between the two models varies with operating time and the difference variation is about 1% in the first 10 days but the variation increases afterwards up to Day 22. Thereafter, the difference remains nearly constant. The maximum variation with time between the two models is no more than 4%. The maximum difference in the daily heat transfer between the two models is approximately 2% for a short heat exchanger to 4% for a long heat exchanger. Therefore, it can be concluded that for simulation of horizontal straight ELHXs, a two-dimensional model can be used with reasonable accuracy. The results also imply that for more sophisticated configurations of horizontal ELHXs such as slinky coil loops for ground source heat pumps, three-dimensional modelling can be performed for a small section (eg one pitch for a slinky loop) instead of a complete length of pipes. Such practice has been implemented previously [11, 12].

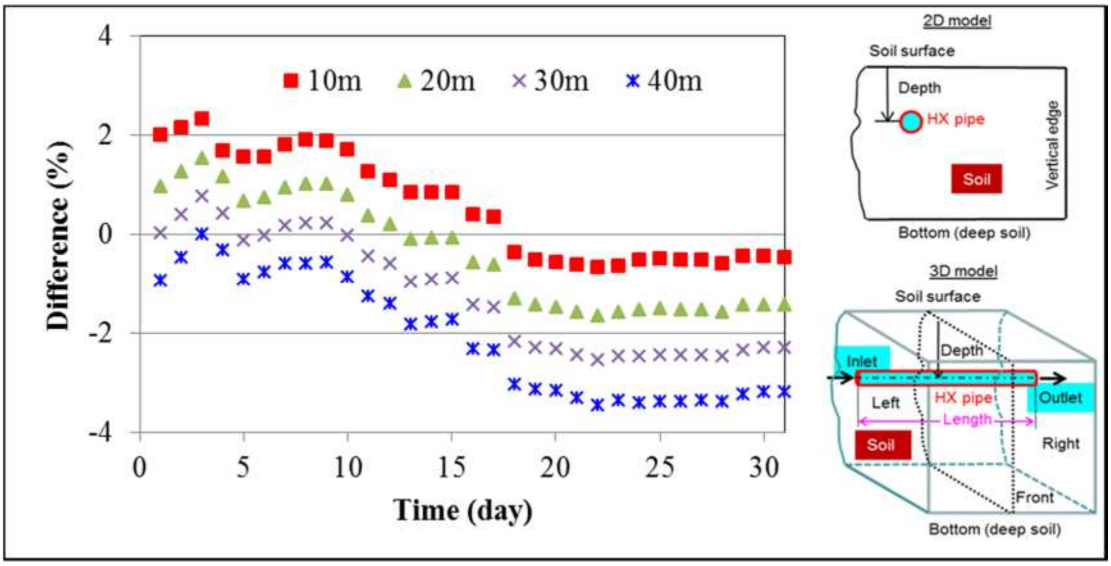

Fig. 13 Comparison between 2D and 3D models for the predicted daily heat transfer for different lengths of ELHX in January

4 Conclusions

A three-dimensional numerical model has been used for simulation of the dynamic thermal performance of ground heat exchangers for ground source heat pumps and tunnel ventilation. The effects of the fluid temperature, flow rate, soil moisture and pipe thermal resistance as well as dynamic interactions between the heat exchanger, soil and ambient environments have been investigated.

Direct thermal and moisture interactions between a heat exchanger, soil and atmosphere have a significant impact on the heat transfer through a heat exchanger. Neglecting the interactions between the heat exchanger, soil and fluid would significantly over predict the thermal performance of a ground heat exchanger in cold winter, by as much as 463% for a 10 m long earth-liquid heat exchanger. The amount of over-prediction for an earth-liquid heat exchanger is much larger than that for an earth-air heat exchanger which can however still be over 100%. A dynamic simulation would be required to provide accurate data for design of a ground source heat pump or earth-air tunnel ventilation system for integration into a building in order to minimise the difference between design and in-use energy performance.

Heat transfer in soil is also influenced by its moisture content and adequate representation of moisture-dependent soil properties is vital for accurate prediction. The level of influence depends on the magnitude of heat transfer. For example, the amount of daily heat transfer of 20 Wh/m through an earth-liquid heat exchanger in soil with a moisture content of 0.22 m^3/m^3 could increase by about 10% if the soil moisture increases to 0.3 m^3/m^3.

The thermal resistance of pipes cannot be ignored in performance simulation and system design of an earth-liquid heat exchanger. The daily heat transfer can be increased by 10% to 12% when the resistance is reduced from the level of plastic pipes to that of surrounding soil. The heat transfer rate through a heat exchanger with a lower resistance is generally higher but could be lower for part of the daytime when the temperature of the working fluid that varies with ambient air increases substantially.

For typical operating conditions, an earth-liquid heat exchanger is more efficient for heat transfer than an earth-air heat exchanger. In other words, a ground source heat pump is more efficient for heating/cooling of supply air than an earth-air tunnel ventilation system coupled with electric heating/cooling.

A three-dimensional model should be used for accurate prediction of the thermal performance of a ground heat exchanger. For a horizontal earth-liquid heat exchanger, the fluid temperature change along the pipe is small and a two-dimensional model may be used for performance evaluation with a maximum difference of less than 4%.

Monthly mean temperature could be used in place of a fluid temperature that varies with ambient air or building load to estimate the heat transfer for continuous operation of a ground source heat pump system with a maximum error of less than 10%. However, for intermittent operation with a fixed schedule, such estimation could incur large errors.

References

[1]. C.S.A. Chong, G. Gan, A. Verhoef, R.G. Gonzalez, P.L. Vidale, Simulation of thermal performance of horizontal slinky-loop heat exchangers for ground source heat pumps, Applied Energy 104 (2013) 603-610.

[2]. G. Mihalakakou, J.O. Lewis, M. Santamouris, The influence of different ground Covers on the heating potential of earth-to-air heat exchangers, Renewable Energy 7 (1996) 33–46.

[3]. G.N. Tiwari, M.A. Akhtar, M.E. Shukla Khan, Annual thermal performance of greenhouse with an earth air heat exchanger: an experimental validation, Renewable Energy 31 (2006) 2432–46.

[4]. O. Ozgener, L. Ozgener, Experimental study of the exergetic performance of an underground air tunnel system for greenhouse cooling, Renewable Energy 35 (12) (2010) 2804–2811

[5]. R.G. Gonzalez, A. Verhoef, P.L. Vidale, B. Main, G. Gan, Y. Wu, Interactions between the physical soil environment and a horizontal ground coupled heat pump, for a domestic site in the UK, Renewable Energy 44 (2012) 141-153.

[6]. O.J. Svec, L.E. Goodrich, J.H.L. Palmer, Heat transfer characteristics of in-ground heat exchangers, Energy Research 7 (1983) 265–278.

[7]. F. Niu, Y. Yu, D. Yu, H. Li, Heat and mass transfer performance analysis and cooling capacity prediction of earth to air heat exchanger, Applied Energy 137 (2015) 211–221.

[8]. V. Bansal, J. Mathur, Performance enhancement of earth air tunnel heat exchanger using evaporative cooling, International Journal of Low Carbon Technologies 4 (2009) 150-158.

[9]. M. Maerefat, A.P. Haghighi, Passive cooling of buildings by using integrated earth to air heat exchanger and solar chimney, Renewable Energy 35 (2010) 2316–2324.

[10]. V.C. Mei, Horizontal ground-coil heat exchanger theoretical and experimental analysis. Oak Ridge National Laboratory Report, ORNL/CON-193, 1986.

[11]. Y. Wu, G. Gan, A. Verhoef, P.L. Vidale, R. Garcia Gonzalez, Experimental measurement and numerical simulation of horizontal-coupled slinky ground source heat exchangers, Applied Thermal Engineering 30(16) (2010) 2574-2583.

[12]. G. Gan, Dynamic thermal modelling of horizontal ground source heat pumps, International Journal of Low Carbon Technologies 8(2) (2013) 95-105.

[13]. M. Santamouris, G. Mihalakakou, C. Balaras, A. Argiriou, D. Asimakopoulos, M. Vallindras, Use of buried pipes for energy conservation in cooling of agricultural greenhouses, Solar Energy 55 (2) (1995) 111–124.

[14]. J. Darkwa, G. Kokogiannakis, C.L. Magadzire, K. Yuan. Theoretical and practical evaluation of an earth-tube (E-tube) ventilation system, Energy and Buildings 43 (2011) 728–736.

[15]. M. Bottarelli, V. Di Federico, Numerical comparison between two advanced HGHEs. International Journal of Low Carbon Technologies **7**(2) (2012) 75-81.

[16]. G. Gan, Dynamic interactions between the ground heat exchanger and environments in earth–air tunnel ventilation of buildings, Energy and Buildings 85 (2014) 12–22.

[17]. G. Gan, Simulation of dynamic interactions of the earth-air heat exchanger with soil and atmosphere for preheating of ventilation air, Applied Energy 158 (2015) 118-132.

[18]. G. Gan, Impacts of dynamic interactions on the predicted thermal performance of earth-air heat exchangers for preheating, cooling and ventilation of buildings,

International Journal of Low Carbon Technologies (2015) doi:10.1093/ijlct/ctv029.
[19]. J. R. Philip, D. A. De Vries. Moisture movement in porous materials under temperature gradients, Trans. Am. Geophys. Union 38 (1957) 222-232.
[20]. V. Gnielinski, New equations for heat and mass transfer in turbulent pipe and channel flow, Int. Chemical Engineering 16 (1976) 359-368.
[21]. ANSYS Inc. FLUENT, Canonsburg, Pennsylvania, 2012.
[22]. REHAU ECOAIR Ground-air heat exchanger system, https://www.rehau.com/download/815550/awadukt-thermo-urun-programi.pdf. (Accessed: November 3, 2016)
[23]. CIBSE, Guide J - Weather, solar and illuminance data, Chartered Institution of Building Services Engineers, London, 2002.
[24]. UK Climate, http://www.metoffice.gov.uk/public/weather/climate/bracknell. (Accessed: April 5, 2013).
[25]. B.J. Cosby, G.M. Hornberger, R.B. Clapp, T.R. Ginn, A statistical exploration of the relationships of soil moisture characteristics to the physical properties of soils, Water Resources Research 20(6) (1984) 682-690.